

Mathieu Ichard *, Olav Hansen[#] and Jens Melheim*

*GexCon AS, Bergen, Norway

[#] GexCon US, Bethesda, MD, USA

1. INTRODUCTION

Highly hazardous chemicals are mainly stored and transported as pressurized liquids at conditions above the saturation pressure. The chemical is said to be sub-cooled with a degree of sub-cooling defined as the difference between the storage pressure and the saturation pressure at the storage temperature. In the case of a failure of containment, the pressurized liquid is released into the ambient atmosphere and it is crossing the vapor pressure saturation curve. The liquid is said to be in a thermodynamically meta-stable state. In this thermodynamic state, the liquid is described as superheated since its temperature, close to ambient, is higher than its normal boiling point. The flashing process which is a rapid boiling process happens and leads to the formation of a two-phase jet with vapor and droplets.

The largest droplets may rain-out on the ground forming a pool that would spread and evaporate. Droplets smaller than a critical size will remain airborne and evaporate as air is entrained into the two-phase jet. The rain-out process may help reducing the maximum concentrations observed downwind of the release point. On the other hand, evaporation from the pool increases the duration of the hazard. Accurate hazard quantifications therefore require a proper prediction of the amount of liquid that may rain-out from the two-phase jet.

In realistic industrial environments with a high degree of confinement and congestion such as offshore platforms and onshore plants, the two-phase jet may impinge on an obstacle. Impingement will increase the percentage of liquid that will rain-out and form a pool on the ground. The FLIE project (Flashing Liquids in Industrial Environments) aimed at studied small and large scale flashing jets. This EU-project was coordinated by GexCon and the experimental tests were realized by the Von-Karman Institute (VKI) and INERIS. During the INERIS FLIE test series, Bonnet (2005), performed in France from March to October 2004, large scale flashing releases of butane and propane were investigated. The experiments consisted of free and impinging flashing jets. One of the main aims of the test series was to get some insight in how impingement at obstacles in the near field of a flashing jet would influence the rain-out percentage.

The main objective of this work is to develop and improve models for flashing releases in the Computational Fluid Dynamics (CFD) 3-D code FLACS. For the time being FLACS has a utility program called FLASH which estimates the location and characteristics of a pseudo-release, accounting for air entrainment, droplet rain-out and evaporation (Salvesen, 1995). The location of the pseudo-source is defined as the location downwind of the release point where all the droplets have evaporated. The actual model cannot handle the influence of the presence of an obstacle on the two-phase flashing jet and subsequent rain-out. In Section 2 the INERIS FLIE experiments are briefly described. Then, in a first step, models for the estimation of the source term at the exit orifice and for the evaluation of the amount of liquid that rains-out on the ground due to jet impingement are presented and the predictions are compared with the experimental observations of the INERIS FLIE experiments. Outputs from the source models are then used to define a pseudo-source in the FLACS code. The pseudo-source in the new FLACS model is located at the point where flashing has occurred. In this work a homogeneous equilibrium model has been implemented in FLACS in order to model the behavior of the two-phase jet. In the last section, the implemented homogeneous equilibrium model is presented and four experimental tests of flashing jets are simulated with the FLACS code. Results for the temperature fields are compared with the experimental data.

2. INERIS FLIE EXPERIMENTS

The INERIS FLIE test series consisted of 94 large-scale flashing jet releases carried out from March to October 2004 by INERIS in France. Two different liquefied gases were used, 64 tests were performed with propane and 30 tests with butane. The aims of the experiments were to get an insight in the properties of flashing jets, droplet characteristics and temperatures, and to investigate the rain-out from two-phase jets impinging on a wall.

The influence of several parameters on the behavior of a flashing jet was investigated. A wide range of degree of sub-cooling was tested. In addition to the vapor pressure of the liquefied gas, 0, 1, 3 or 6 bar over-pressure in the storage tank was added using nitrogen. Circular and rectangular orifices were used. Circular orifices of diameters ranging from 2 mm to 25 mm as well as rectangular and square orifices were used. Retention tanks were placed on weight indicators below the jet and measured the rain-out. Impingement distances of 0.83 m, 1.60 m and

* *Corresponding author address:* Mathieu Ichard, GexCon AS, Fantoftvegen 38, 5892, Bergen, Norway +47 40554068, e-mail: mathieu@gexcon.com

2.57 m between the exit orifice and the wall were tested. As the tests were at large-scale environmental conditions varied from one test to another as well as during several tests. The tests were performed outside and the ambient temperature, humidity, wind velocity and wind direction were measured and reported.

In addition to the stagnation conditions, i.e. temperature and pressure inside the tank, and exit conditions, i.e. temperature and pressure of the liquid 10 cm upstream of exit orifice, many other parameters were measured during the experiments. The mass flow rates were estimated measuring the weight of the storage tank during the releases. The accuracy of the weight measurements was around hundred grams. For propane the release rates varied from 0.044 to 2.3 kg/s and for butane from 0.13 to 2.1 kg/s. The temperature at several positions along the jet axis as well as on the obstacle in the case of impinging jets, was measured with thermo-couples. For butane and propane, there were six temperature measurement distances, in the longitudinal direction (down to 6.5 m from exit location) and for each of these, measurements were reported at three positions in the vertical direction. The diameter, axial velocity and vertical velocity of droplets were measured using Phase Doppler Anemometer (PDA), a non-intrusive optical measurement technique. A precise description of the PDA measurement device can be found in the literature, e.g. Albretch (2003). A double PDA system was built in order to simultaneously measure two components of the droplet velocity vector (axial and vertical) and the droplet diameter.

Figure 1 shows number-based probability density functions for the droplets diameter, axial velocity and vertical velocity obtained during one of the INERIS FLIE tests. During this test propane was released through a circular orifice with a diameter of 2 mm. The pressure inside the storage tank was 2.0 bar above the vapor pressure at the storage temperature. Droplet characteristics were measured at seven positions downstream along the center-line axis of the jet from $x/D = 20$ down to $x/D = 195$. The probability distributions for the droplet diameter do not show any strong variations along the center-line axis of the jet. The axial velocity of the droplets decreases when moving downstream. The vertical velocity of the droplets is almost constant with increasing distance downstream and the mean arithmetic value is around 0 m/s.

Up to six retention tanks were used to evaluate the amount of liquid that rains-out for both impinging and free flashing jets. Each of the retention tanks has a surface area of 1 m^2 and a capacity of 0.2 m^3 . The retention tanks were placed on weight indicators with a precision of a hundred grams. For free flashing jets of propane INERIS reported that no pool formation

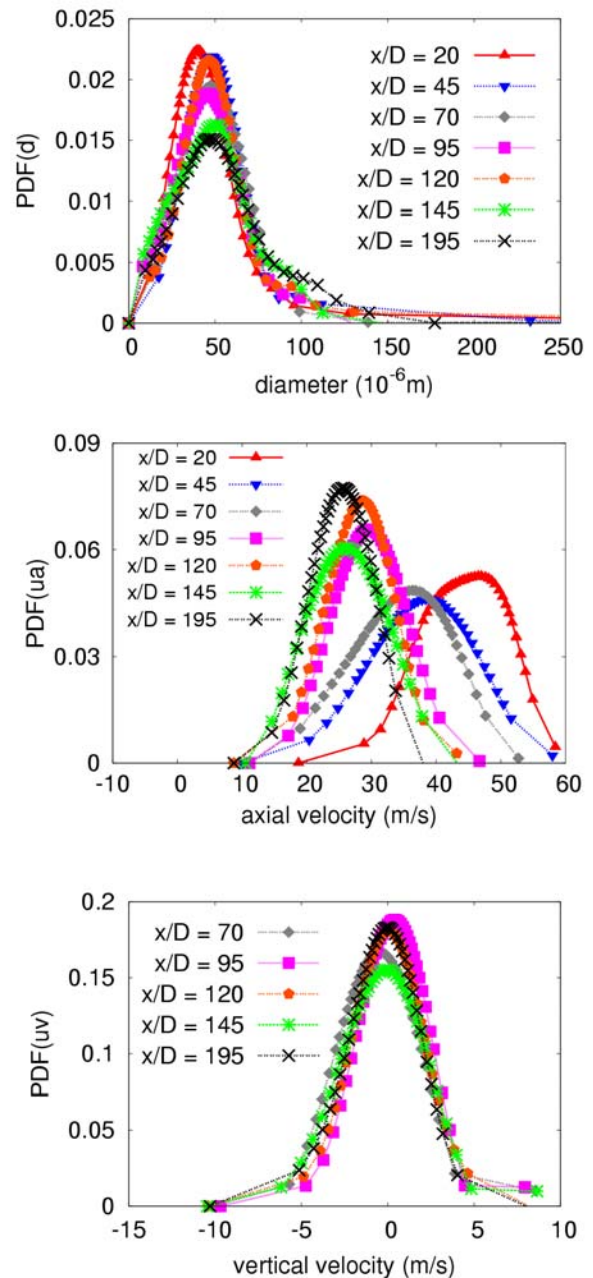


Figure 1 – Probability Distribution Functions (PDF) for droplets diameter, axial velocity and vertical velocity along the center-line axis of a flashing propane jet.

took place. For butane, a maximum value of 10 % for the rain-out percentage has been observed in some tests.

3. COMPUTATIONS OF THE SOURCE TERMS

Toxic industrial chemicals are mainly stored and transported as pressurized liquids. Based on the storage conditions the degree of sub-cooling can be defined as:

$$\chi = \frac{P_0}{P_s(T_0)} \quad (1)$$

where P_0 is the stagnation pressure and $P_s(T_0)$ is the saturation pressure corresponding to the inlet stagnation temperature, T_0 . When released into the atmosphere, the liquid will suddenly reach a meta-stable thermodynamic state below the vapor pressure curve. In order to reach a more stable thermodynamic state, the liquid rapidly boils, it flashes. The initial liquid stream is broken-up into droplets and ligaments by the combined effects of thermodynamic and mechanical break-up processes. The thermodynamic break-up process, i.e. shattering of the jet, is due to the rapid boiling of the liquid and the subsequent dynamic expansion of vapor bubbles. The mechanical break-up of the liquid jet is caused by shear forces. Efficiency of the mechanical break-up process, i.e. the size of the droplets and ligaments, is driven by the jet velocity. The higher the jet velocity is relative to the surrounding atmosphere the more efficient the process is. The droplets can either remain airborne in the jet or rain-out on the ground. Figure 2 illustrates a flashing jet impinging on an obstacle.

3.1 Mass Flow Rate at the exit orifice

Failures of storage containments can lead to releases of the stored material through a sharp edge orifice or through a pipe. From the work of Fauske (1988) the mass flow rates of sub-cooled liquids through sharp edge orifices were well predicted by the following expression:

$$G = C_D \sqrt{2\rho_{l_0}(P_0 - P_e)} \quad (2)$$

where P_e is the pressure at the exit orifice, ρ_{l_0} is the density of the liquid at the storage conditions and C_D is the discharge coefficient set to a value of 0.62.

In the case of a release through a pipe connecting the liquid part of the storage tank to the atmosphere, it has been observed that the sub-cooled liquid may flash inside the pipe before reaching the exit orifice (Leung, 1990). If the liquid flashes inside the pipe the flow is two-phase before the exit orifice and the mass flow rate cannot be estimated by

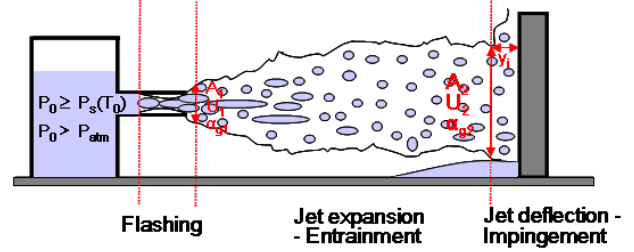


Figure 2 – Simplified view of an impinging flashing jet

Equation (2). Assuming that the occurrence of flashing is controlled by the degree of sub-cooling defined by the stagnation conditions, the model of Leung (1990) should predict the mass-flow rate for releases through pipes, flashing or non-flashing before the exit.

In the model of Leung, a suitable correlating parameter is first defined:

$$\omega = \rho_{l_0} C_p T_0 P_s(T_0) \left(\frac{g_{vl_0}}{h_{vl_0}} \right)^2 \quad (3)$$

where ρ_{l_0} is the liquid density at stagnation condition, C_p is the liquid specific heat at constant pressure, g_{vl_0} is the difference in specific volume between the vapor and liquid phase at stagnation condition and h_{vl_0} is the difference between vapor and liquid phase at stagnation condition. The following inequality on ω separates the initial stagnation conditions into high sub-cooled and low sub-cooled stagnation conditions:

$$\eta_s \geq 1 - \frac{1}{2\omega} \quad \eta_s = \frac{P_s(T_0)}{P_0} \quad (4)$$

In the low sub-cooling region, where the Equation (4) is satisfied, the liquid attains flashing before reaching the exit orifice. The two-phase mass flow rate is then predicted through the following equation:

$$G^* = \frac{\left\{ 2(1-\eta_s) + 2 \left[\omega \eta_s \ln \left(\frac{\eta_s}{\eta} \right) - (\omega-1)(\eta_s-\eta) \right] \right\}^{0.5}}{\omega \left(\frac{\eta_s}{\eta} - 1 \right) + 1} \quad (5)$$

where η is the ratio of the exit orifice pressure and the stagnation pressure, G^* is a non-dimensional mass flow rate expressed by:

$$G^* = \frac{G}{\sqrt{P_0 \rho_0}} \quad (6)$$

Since the flow is two-phase, choking conditions may occur at the exit. The critical pressure ratio, η_c , is found by solving the equation:

$$\frac{\left(\omega + \frac{1}{\omega} - 2\right)}{2\eta_s} \eta_c^2 - 2(\omega - 1)\eta_c + \omega\eta_s \ln\left(\frac{\eta_c}{\eta_s}\right) + \frac{3}{2}\omega\eta_s - 1 = 0 \quad (7)$$

For highly sub-cooled cases, flashing does not occur before the exit location and no vapor is formed. The release is a single, liquid phase release and the mass flow rate is predicted by the Bernoulli-type Equation (2).

Based on the stagnation conditions, T_0 and P_0 , and the diameters of the circular orifices, the predictions of the model described previously are compared with the experimental data from the INERIS FLIE test series. The comparison is shown on Figure 3. The 30% error lines are shown on the plot. Two exit pressures namely the saturation pressure at the stagnation temperature and the atmospheric pressure are used to evaluate the mass flow rate with Equation (2). For propane, large differences in the predicted mass flow rates are obtained with the two different exit pressures. Using the saturation pressure as exit pressure leads to an under-estimation of the mass flow rates whereas with the atmospheric pressure as exit pressure, the mass flow rates are over-estimated. Moreover, in the INERIS FLIE test series an adiabatic pipe of length 30 m and of diameter 50 mm has been used to link the bottom part of the tank to the exit orifice. Therefore, since friction is not taken into account in the model, the predicted mass flow rates should be greater than the measured ones.

It can also be noticed that as the degree of sub-cooling, χ , increases the differences between the mass flow rates obtained with the two different exit pressures is decreasing and the predictions become gradually more accurate. From the 38 cases considered in the comparison, the model predicts flashing before the exit for only one case. This case corresponds to a release of propane through an orifice of diameter 25 mm with a degree of sub-cooling of $\chi = 1.05$. The measurements in the liquid phase of the pressure and the temperature 10 cm before the exit orifice do show that flashing is occurring inside the pipe. The measured pressure is

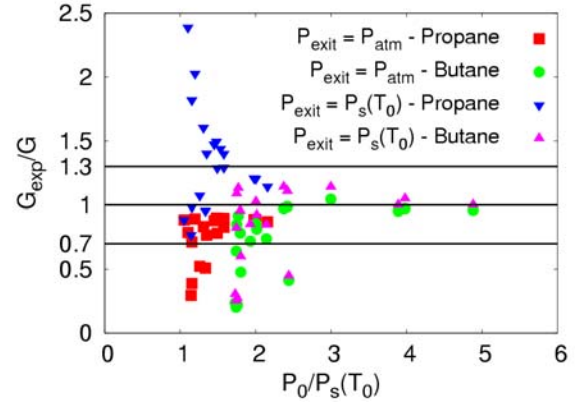


Figure 3 – Predictions of the mass flow rates at the exit orifice for 38 flashing releases of propane and butane through circular orifices.

below the saturation pressure at the measured temperature. However, it can be noticed that nine points are below the 0.7 line meaning that the predicted mass flow rate is over-estimating the data by more than 30%. For these nine cases the exit diameter is greater than or equal to 20 mm and flashing may have occurred inside the pipe. The measured temperatures and pressures 10 cm upstream of exit orifice show reductions of 1 bar and 10 °C compared to stagnation conditions. These reductions are not observed for orifices with diameters smaller than 20 mm.

The error in the mass flow rate and the difference between the pressure and saturation pressure 10 cm upstream of the exit orifice are increasing with increasing orifice diameter. It can be concluded that in addition to the degree of sub-cooling defined by the stagnation conditions, the geometry of the exit orifice has an influence on the occurrence of flashing inside the pipe.

3.2 Rain-out induced by jet impingement

A semi-empirical approach is used to compute the removal of droplets from a two-phase jet impinging on a wall. In this simplified approach, the entire process is divided into different regions: flashing, jet expansion, jet deflection and jet impingement. This sequential approach is extensively described in Chiang (2000). The positions of the different regions are shown on Figure 2. It is assumed that the mass flow rate at the exit orifice is known and that all the material is in the liquid phase. In addition, we assume that the flashing phenomenon happens over a distance of one diameter after the exit orifice. During flashing the liquid boils by extracting energy

from itself. A simple energy balance gives the mass fraction of vapor x_g after expansion due to flashing:

$$x_g = \frac{C_p(T_e - T_{nbp})}{L} \quad (8)$$

where C_p is the liquid specific heat capacity at constant pressure of the liquid, T_e is the exit temperature, T_{nbp} is the normal boiling point of the substance and L is the latent heat of vaporization of the substance. Based on Equation (2) and the comparison with experimental data shown on Figure 3, the pressure at the exit is taken to be the atmospheric pressure. Therefore, there is no further jet acceleration after the exit orifice due to depressurization. No air entrainment is assumed during the flashing process, the conservation of mass leads to the following expression for the cross area A_1 of the jet after flashing:

$$A_1 = \frac{G}{\rho_m U_1} \quad (9)$$

where U_1 is equal to the exit velocity at the exit orifice, G is the mass flow rate and ρ_m is the density of the mixture after flashing.

The next step is to determine the position downstream where the jet is influenced by the presence of the wall. At this position the jet starts to deflect and its center-line velocity is 98% of the center-line velocity of a free jet at the same distance from the exit orifice. Estimation of the deflection position is based on the experimental work of Giralt (1977). Giralt measured decay velocities of an air jet for different nozzle-plate separation and two different exit diameters, 28.58 mm and 31.75 mm. Based on the exit conditions the jet Reynolds number varied from 30 000 to 80 000. From their experimental data, Giralt derived the following correlation for the location of the deflection point y_i :

$$\begin{aligned} \frac{y_i}{D_1} &= 1.2 \quad \text{for} \quad \frac{l_p}{D_1} < 6.8 \\ \frac{y_i}{D_1} &= 0.153(1 + \frac{l_p}{D_1}) \quad \text{for} \quad \frac{l_p}{D_1} > 6.8 \end{aligned} \quad (10)$$

where y_i is defined as the distance between the obstacle and the deflection point and l_p is the

distance between the exit orifice of diameter D_1 and the obstacle. It is worth mentioning that, to the author's knowledge, Equation (10) has only been validated for the experimental conditions of Giralt.

The properties of the jet at the deflection position need to be estimated. The jet is expanding with a 5° angle, (Salvesen, 1995), so that the diameter D_2 of the jet at the deflection position can be computed by:

$$\frac{D_2}{D_1} = 1 + \frac{2(l_p - y_d)}{D_1} \tan(5^\circ) \quad (11)$$

Jet expansion is mainly driven by the rate at which air is entrained into the jet. As for the estimation of the velocity U_1 after flashing, the variation of the velocity is averaged across the jet area. The velocity varies only in the axial direction. Writing the conservation of momentum for the two-phase jet over a 1-D control volume extending from the position where flashing had occurred to the position where the jet starts to deflect, leads to the following expression, (Fluke, 1983):

$$\rho_m A_1 U_1^2 = \rho_m A_{2m} U_2^2 + \rho_a (A_2 - A_{2m}) U_2^2 \quad (12)$$

where ρ_a is the density of dry air, U_2 is the velocity of the jet at the deflection position and A_{2m} is the jet area at the deflection position excluding air. Applying the conservation of mass we obtain:

$$U_1 = G / (\rho_m A_1) \quad (13)$$

and:

$$U_2 = G / (\rho_m A_{2m}) \quad (14)$$

and substituting these expressions for U_1 and U_2 in Equation (12) the area A_{2m} can be evaluated and the velocity U_2 computed. In the previous set of equations the density of the mixture, ρ_m , containing air, liquid droplets and vapor needs to be estimated. Similar to the velocity, the mixture density is averaged over the cross area of the jet. The mixture density is varying in the axial direction due to air entrainment and droplets evaporation. The density of the mixture is influenced by the evaporation of the droplets. In this work, the homogeneous equilibrium model, (Kukkonen, 1994, Shearer, 1979), has been implemented. In this model the droplets, and the

surrounding gas phase are assumed to be in thermodynamic equilibrium and the droplets are homogeneously distributed over the jet cross area.

The final step, concerns the estimation of both a critical droplet diameter and a representative mass-based droplets diameter distribution. A Rosin-Rammler cumulative distribution function for the droplet diameters has been used:

$$F_m(d) = 1 - \exp\left[-\left(\frac{d}{\delta}\right)^n\right] \quad (15)$$

Based on the droplet measurements performed during the INERIS FLIE experiments, mass median diameter of $156 \cdot 10^{-6}$ m and $235 \cdot 10^{-6}$ m for propane and butane respectively and values of $n = 4.59$ and $n = 5.05$ for the parameter n in Equation (15) for propane and butane, respectively, have been used. These values have been found to be representative of the experimental conditions tested in the INERIS FLIE experiments. The rain-out fraction is then expressed by:

$$f = (1 - F_m(d_c))(1 - x_g) \quad (16)$$

where d_c is the critical droplet diameter. Equation (16) means that droplets with a diameter greater than the critical diameter d_c impinge on the obstacle and rain-out. Estimation of the critical droplet diameter is based on the concept of droplet response time to changes in flow velocity. A time scale associated with the turbulent eddies located between the deflection position and the wall can be estimated by:

$$\tau_f = \frac{D_2}{U_2} \quad (17)$$

If the response time of a droplet is greater than the time scale τ_f the droplet will not be able to follow the mean flow and will impact on the obstacle. The response time of a droplet is expressed as, (Crowe, 1998):

$$\tau_d = \frac{\rho_d d^2}{18\mu_c} \quad (18)$$

where μ_c is the viscosity of the surrounding air. The ratio of the time scale of the turbulent eddies and the response time of a droplet gives the Stokes number:

$$St = \frac{\tau_d}{\tau_f} \quad (19)$$

If the Stokes number is less than one, the response time of the droplet is much less than the characteristic time of the flow field. The droplet will then be able to respond to changes in flow velocity. On the other hand, if the Stokes number is much larger than one, the trajectory of the droplet will not be affected by the change in fluid velocity and direction. The droplet will move independently of the flow field. Experimental results by Yang (1995) and numerical simulations of particle concentration in a wake, (Tang, 1992), show that particles with a Stokes number of around one concentrate at the edges of the vortex structures. Thus, the particles are following nearly exactly the turbulent eddies. For Stokes numbers close to ten the particles start to move independently of the turbulent structures. Particles with a Stokes number of hundred are not affected by the turbulent eddies and move independently of the changes in the flow field. Therefore, we may assume that a critical Stokes number exists and is expressed as:

$$St_c = \frac{\rho_d d_c^2}{18\mu_c \tau_f} \quad (20)$$

The critical droplet diameter can be estimated from the previous equation. The critical Stokes number has been estimated from the INERIS FLIE data and found to be $St_c = 70$.

Table 1 presents rain-out predictions compared to the data from the INERIS FLIE experiments. For each of the tests the distance between the exit orifice and the obstacle as well as the degree of sub-cooling are mentioned. In the tests presented in Table 1, propane and butane were released through a circular orifice of

Specie	$P_0/P_s(T_0)$	Distance (m)	Rain-out		
			Data	Predictions	
				MFR _{exp}	MFR _{comp}
Propane	1.02	0.83	11%-12%	13%	18%
Butane	2.0	1.6	31%-39%	25%	33%
Butane	1.78	1.6	31%-39%	22%	26%
Butane	5.0	1.6	40%-50%	45%	46%
Butane	3.0	1.6	36%-45%	49%	48%
Butane	2.12	0.83	40%-50%	64%	75%

Table 1 – Comparisons between predicted and observed rain-out percentages for different degrees of sub-cooling and different impingement distances.

diameter 10 mm. Predictions obtained with the computed mass flow rates (MFR_{comp}) and with the experimental data for the mass flow rates (MFR_{exp}) are shown. In the experimental tests it was observed that flashing jets of butane gave more rain-out than flashing jets of propane. This is also predicted by the model. For the same impingement distance, the rain-out increases when the degree of sub-cooling increases. The model is also able to predict this feature of flashing impinging jets. The amount of rain-out decreases when the distance between the exit orifice and the wall increases. One can note that the predictions of rain-out obtained with the computed mass flow rate (see Section 3.1) are over-estimating the rain-out calculated with the experimental mass flow rates. This is due to the fact that the computed mass flow rates are over-estimating the real mass flow rates. It is observed that the model does over-estimate the rain-out for a wall distance of 0.83 m and does under-estimate it for low degree of sub-cooling; around 2.0; with wall distances of 1.6 m. This can be seen as a limitation of the simplified approach developed. More detailed computations of the two-phase jet, droplets properties and droplets interactions with the obstacle would be needed to improve the predictions.

4. 3D SIMULATIONS WITH FLACS

Flashing jets of propane and butane are simulated with the 3D-CFD code FLACS. The temperature field obtained from the 3D simulations is compared and validated against the temperature data of the INERIS experiments. The source models described in sections 3.1 and 3.2 are used to estimate the mass flow rate, the cross area of the jet and the vapor fraction after flashing. These values are used as input in the CFD code to define the two-phase release.

The FLACS CFD model was developed in the early 1980s to simulate gas explosions in offshore platforms. The conservation equations are solved on a Cartesian grid using a finite volume method. The $k-\epsilon$ turbulence model is used to close the equations for fluid motion. Hjertager (1985, 1986) describe the basic equations used in the FLACS model. A distributed porosity concept is implemented in FLACS to handle complex geometries. The porosity of a grid volume is represented as a fractional blockage of each grid volume and each face of the grid with sub-grid obstacles. Turbulence production terms are parameterized for sub-grid objects (Arntzen, 1998). Some modifications to the standard $k-\epsilon$ model in FLACS have been made for atmospheric boundary layer turbulence and dispersion applications (Hanna, 2004, 2009 and Dharmavaram, 2005). At the upwind boundary of the domain, vertical profiles of wind

speed and direction, temperature, turbulent kinetic energy, and eddy dissipation rate are calculated by the FLACS model based on the specification of the wind speed at a certain reference height, and the specification of Pasquill stability class (A to F) or Monin-Obukhov length and surface roughness length. FLACS was validated against field experiments involving dense gas and passive gas releases (the Kit Fox, MUST Prairie Grass and EMU experiments, Hanna, 2004) FLACS was also used to investigate hypothetical and real passive and dense gas dispersion cases in cities and industrial areas (Flaherty, 2007, Hanna, 2009).

In 3D simulations of hazardous flashing jets dispersion it is of crucial importance to model the behavior of the droplets. Due to the presence of the droplets, the flashing jet behaves as a heavy jet. At the initial stage of the release, most of the mass of the jet is contained in the liquid phase which has a higher density than the gas phase. As the cloud is transported downstream, it cools down because the droplets are evaporating. The cooling effect increases the bulk density of the jet. The homogeneous equilibrium model has been implemented in the FLACS code in order to account for the processes of droplets evaporation and cooling of the jet. Kukkonen (1994) gives a detailed and comprehensive description of the physics contained in the model. The homogeneous equilibrium model assumes that the droplets are homogeneously statistically distributed both spatially and in size. In the homogeneous equilibrium approach the mixture of vapor, liquid droplets and air is modeled as a heavy mixture with, at a given point in space and time, one characteristic temperature and velocity. The liquid and gas phases are assumed to be in thermodynamic equilibrium at the characteristic temperature. From the Dalton's law of partial pressures, the partial pressure of the chemical substance is:

$$P_g = \alpha_g * P_{atm} \quad (21)$$

Thermodynamic equilibrium implies that the partial pressure of the chemical is the saturation pressure at the mixture temperature. Vapor pressures are computed with the Wagner equation (Poling, 2000). The cooling process can be understood in the following way: as air is entrained inside the jet, the volume fraction of the contaminant vapor is decreasing, the dilution effect, and so does the vapor pressure. Since the vapor pressure is decreasing, the mixture temperature must also decrease. The conservation of enthalpy for the mixture of dry air, vapor and liquid droplets must be satisfied as the temperature of the cloud decreases. The conservation of enthalpy can only be achieved if the liquid

vaporizes and extract the required amount of latent heat of vaporization to reach equilibrium. When all the liquid has evaporated, air entrainment brings the mixture temperature to ambient temperature.

Four INERIS FLIE tests, one with propane and three with butane, were simulated with the FLACS model. The temperature along the jet center line is compared with experimental data obtained in the four tests. Test P1 is a release of propane through a circular orifice of diameter 10 mm and the degree of sub-cooling in the storage tank was $\chi = 1.03$. The computed mass flow rate with the model described in Section 3.1 is 1.37 kg/s. This predicted mass flow rate is 25% higher than the observed mass flow rate. After flashing, the volume fraction of vapor is 0.995 and the area of the jet $7.0 \cdot 10^{-3} \text{ m}^2$. These parameters are used to define the two-phase release in the 3D FLACS code. Additional parameters concern the ambient temperature, 24 °C, the wind speed, 2 m/s and the Pasquill stability class was set to neutral. Tests B1, B2 and B3 were releases of butane through a circular orifice of 10 mm. The degrees of sub-cooling in the storage tank were 1.75, 2.44 and 4.0 for test B1, B2 and B3, respectively. The computed mass flow rates were 0.81 kg/s, 1.03 kg/s and 1.37 kg/s for tests B1, B2 and B3, respectively. The predicted mass flow rates were over-estimating the data by 15%, 2% and 3% for tests B1, B2 and B3, respectively. For test B1, after flashing the volume fraction of vapor was 0.977 and the jet area $3.0 \cdot 10^{-3} \text{ m}^2$. For test B2, the volume fraction of vapor was 0.98 and the jet area $3.0 \cdot 10^{-3} \text{ m}^2$ after flashing. For test B3, after flashing the volume fraction of vapor was 0.977 and the jet area $3.0 \cdot 10^{-3} \text{ m}^2$. The ambient temperature was 23 °C for both tests B1 and B3 and 25 °C for test B2. The wind speed was 2 m/s at 10 m and the Pasquill stability class was set to neutral for all tests.

Figure 4 shows the comparison of simulated and observed temperature profiles along the center line of the jets for the four tests described above. For the propane test, the thermo-couples were saturated at the value of -50 °C. However, even if the thermo-couples have been saturated, it can be observed that the temperature is going below the normal boiling of propane due to the evaporation of liquid droplets. In the simulations the temperature goes down to -70 °C, i.e. 30 °C below the normal boiling point of propane. In the experiment the propane droplets evaporate over a shorter distance compared to the simulation. The temperature along the jet center-line returns to ambient faster than that in the simulation. This difference might be due to the over-estimation of the mass flow rate. For the butane tests experimental data are of better quality. The decrease of temperature below the normal boiling point of butane is well predicted in the FLACS simulations. It can also be noted that in both simulations and experiments,

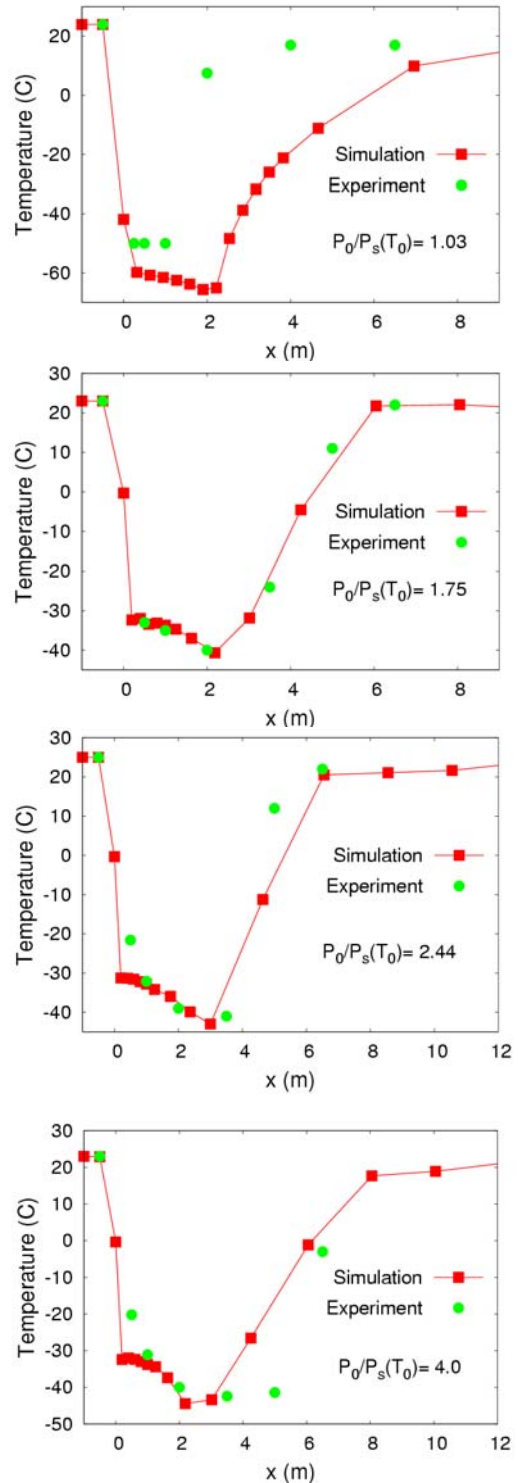


Figure 4 – Temperature profiles along the center-line axis of flashing jets of propane and butane. From top to bottom: Test P1, Test B1, Test B2 and Test B3.

the minimum mixture temperature is obtained when all the droplets have evaporated. This has also been observed by Kukkonen (1994). The effect of the degree of sub-cooling on the distance needed by the droplets to evaporate can also be noticed. When the degree of sub-cooling increases the distance needed by the droplets to evaporate increases. For the highest degree of sub-cooling tested, the FLACS code under-estimates the evaporation distance.

5. CONCLUSION

An approach to model the rain-out of an impinging flashing jet has been presented and validated against the INERIS FLIE experiments. Flashing jets of propane and butane with different degrees of sub-cooling have been investigated during the FLIE experiments. In these experiments a pipe with a 50 mm diameter and of 30 m in length has been used to link the bottom part of the storage tank to the exit orifice.

The model of Leung (1990) has been used to estimate the mass flow rate at the exit orifice. Comparison with experimental data show that the accuracy of the predictions improves when the degree of sub-cooling increases. In addition to the degree of sub-cooling, several diameters for the exit orifice have been tested in the experiments. Flashing of the substance may happen in the pipe before the exit orifice. The occurrence of flashing does not only depend on the degree of sub-cooling but also on the diameter of the exit orifice. A more complex model predicting the occurrence of flashing inside the pipe as well as the volume fraction of vapor at the exit orifice is needed.

A sequential approach used to estimate the percentage of liquid that rains-out after jet impingement has been presented. This approach is based on the work by Chiang (2000). The predictions were compared with experimental data of the INERIS FLIE experiments. The rain-out is greater for butane than for propane, increases with increasing degree of sub-cooling and decreases with increasing distance of impingement. All of these characteristics observed during the experiments are predicted by the model. The predictions obtained using the rather coarse approach show a promising correlation with experimental results, keeping in mind significant elements of uncertainty in rain-out observations and in the release rate estimations.

Information from the source models, i.e. mass flow rate and percentage of liquid that rains-out, are used to define a flashing jet in the 3D CFD code FLACS. Flashing jets of butane and propane were simulated with the FLACS code. The evaporation rate was determined by a homogeneous equilibrium model. Comparisons of the temperature field along

the center-line axis of four two-phase jets with experimental data show a satisfactory agreement.

A complete simulation of an impinging flashing jet release can be performed in the 3D CFD code FLACS. A pool model is available in FLACS, and the mass fraction of liquid that rains-out can be used to define an input mass flow rate for this model. Future work will investigate the concentrations observed downwind of an impinging flashing jet.

6. ACKNOWLEDGEMENTS

This research has been sponsored by a PhD grant and by the CLIMIT program of the Norwegian Research Council. The authors would like to thank INERIS for the generation of the INERIS FLIE data and Steve Hanna and sponsors for cooperation in relevant projects supported by the Defense Threat Reduction Agency (DTRA) and the Department of Homeland Security/Transportation Security Administration (DHS/TSA).

7. REFERENCES

- Albretch, H.E., Borys, M., Damaschke, N., Tropea, C., 2003: Laser Doppler and Phase Doppler Measurement Techniques, *Springer-Verlag*.
- Arntzen, B.A., 1998: Modelling of turbulence and combustion for simulation of gas explosions in complex geometries. *PhD thesis*, NTNU, Trondheim, Norway. ISBN 82-471-0358-3.
- Bonnet, P., Bricout, P., Jamois, D., Meunier, P., 2005: Description of experimental large scale two-phase release tests, *INERIS report No. 41508*.
- Chiang, H.W., 2000: A model for the removal of water droplet aerosols from a flashing jet impinging onto a plate. *J. Aerosol Sci.*, Vol. **31**, No. **9**, pp. 999-1014
- Crowe, C., Sommerfeld, M., Tsuji, Y., 1998: Multiphase flows with droplets and particles, *CRC Press LLC*. ISBN 0-8493-9469-4.
- Dharmavaram, S., Hanna, S.R., Hansen, O.R., 2005: Consequence analysis – using a CFD model for industrial sites. *Process Safety Progress* **24**, pp. 316-327.
- Fauske, H.K., Epstein, M., 1988: Source term considerations in connection with chemical accidents and vapour cloud modelling. *J. Loss Prev. Process Ind.*, Vol. **1**, pp. 75-83
- Flaherty, J.E., Allwine, K.J., Brown, M.J., Coirier, W.J., Ericson, S.C., Hansen, O.R., Huber, A.H., Kim, S., Leach, M.J., Mirocha, J.D., Patriak, G., Senocak, I., 2007, Evaluation study of building-resolved urban dispersion models, Paper 10.2 at Seventh Symposium on the Urban Environment, 10-13 September 2007, American

- Meteorological Society; available online at <http://www.ametsoc.org>.
- Fluke, R.J., Skears, J., Jamieson, T.J., Csillag, E.G., Fung K., 1983: Fission product washout by two-phase flashing jets. *Proc. CSNI Specialist Meeting on Water Reactor Containment Safety*, Toronto, ON, Vol. I, pp. 3.1-3.12.
- Giralt, F., Chia C.-J., Trass, O., 1977: Characterization of the impingement region in an axisymmetric turbulent jet. *Ind. Eng. Chem. Fundam.* **16**, pp. 21-28
- Hanna, S.R., Hansen, O.R., Dharmavaram, S., 2004: FLACS air quality CFD model performance evaluation with Kit Fox, MUST, Prairie Grass and EMU observations. *Atmos. Environ.* **38**, pp. 4675-4687.
- Hanna, S.R., Hansen, O.R., Ichard, M., Strimaitis, D., 2009: CFD model simulation of dispersion from chlorine railcar releases in industrial and urban areas. *Atmos. Environ.* **43**, pp. 262-270
- Hjertager, B.H., 1985: Computer simulation of turbulent reactive gas dynamics. *J. Model. Identification Control* **5**, pp. 211-236
- Hjertager, B.H., 1986: Three-dimensional modeling of flow, heat transfer, and combustion. Handbook of Heat and Mass Transfer. *Gulf Publishing Company*, PO Box 2608, Houston, TX, pp. 304-350 (Chapter 4).
- Kukkonen, J., Kulmala, M., Nikmo, J., Vesala, T., Webber, D.M., Wren, T., 1994: The homogeneous equilibrium approximation in models of aerosol cloud dispersion. *Atmos. Environ.* Vol. **28**, No. 17, pp. 2763-2776
- Leung, J.C., 1990: Two-phase flow discharge in nozzles and pipes – a unified approach. *J. Loss Prev. Process Ind.*, Vol. **3**, pp. 27-32
- Poling, B.E., Prausnitz, J.M., O'Connell, J.P., 2000: The properties of gases and liquids, fifth edition. *McGraw-Hill Professional*, ISBN 00-701-1682-5
- Salvesen, H.C., 1995: Modelling release of liquefied gas under high pressure. *CMR-95-F20062*, Christian Michelsen Research, Fantoftvegen 38, PO Box 6031, N-5892 Bergen, Norway.
- Shearer, A.J., Faeth, G.M., 1979: Evaluation of a locally homogeneous model of spray evaporation, *NASA Contractor Report 3198*.
- Tang, L., Wen, F., Yang, Y., Crowe, C.T., Chung, J.N., Troutt, T.R., 1992: Self organizing particle dispersion mechanism in free shear flows, *Phys. Fluids A*, **4**, 2244.
- Yang, Y., Crowe, C.T., Chung, J.N., 1995: Experiments on particle dispersion in a plane wake, *WSU MMO Rep.* 95-7.